Novel Deconvolution Kernel for Extended Depth-of-Field Microscopy with a High-Speed Deformable Mirror

William J Shain, Nicholas A Vickers, Bennett B Goldberg, Thomas Bifano, and Jerome Mertz
[1] Photonics Center, Boston University, 8 Saint Mary's Street, Boston, MA 02215
[2] 5Searle Center for Advanced Learning and Teaching, Northwestern University, 627 Dartmouth Place Evanston, IL 60208
**Corresponding author: shaine@bu.edu*

Abstract: A deformable mirror is used to scan the focal plane during the camera exposure, obtaining extended depth-of-field. A deconvolution kernel is approximated for a given scan depth and used to de-blur the image.
OCIS codes: (180.2520) Fluorescence microscopy; (110.1080) Active or adaptive optics; (100.1830) Deconvolution

1. Introduction

In many fluorescence microscopy applications it is important to image large volumes at high speed. In brain imaging, for example, neuronal signals can vary at millisecond timescales [1], with communicating neurons often separated by hundreds of microns. Imaging such fast dynamics over extended volumes presents a challenge for standard wide-field fluorescence microscopes [2]; while cameras are available with kilohertz frame rates, these provide only 2D snapshots. Fortunately, quasi 3D imaging can be obtained by extending the depth of field (DOF). We describe a simple, light-efficient technique for achieving fast, single-shot extended depth-of-field (EDOF) with a deformable mirror (DM) configured as an add-on to a commercial microscope. The raw images produced by our device, while revealing all-in-focus information, also feature out-of-focus haze. This haze is removed by deconvolution using both an exact and approximated filter function derived directly from the microscope 3D optical transfer function (OTF).

2. Figures and tables

Our setup is illustrated in Fig. 1. A conventional epifluorescence microscope projects a magnified image ($M=f_1/f_{obj}$) of the sample onto an intermediate image plane, where a camera normally resides. In our case, the camera is set back and the intermediate image plane is re-imaged onto the new camera plane using relay lenses f_2 and f_3, and a tilted DM is located in a plane conjugate to the microscope pupil plane. The purpose of tilting the DM is to avoid the use of a beam-splitter and thus maximize light efficiency.

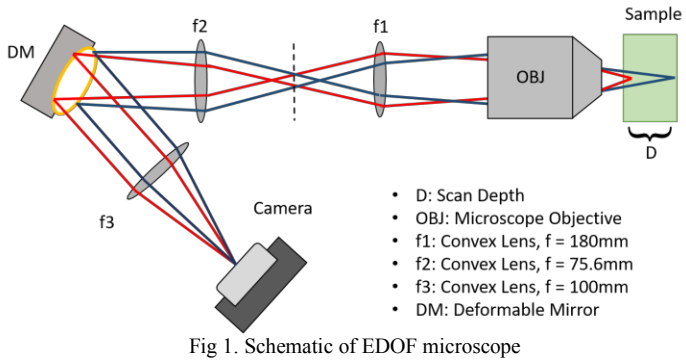

Fig 1. Schematic of EDOF microscope

Focus control is obtained by applying a parabolic shape to the DM, leading to an axial shift of the focal plane in the sample given by $Z = nf_2^2/(M^2 f_{DM})$ where f_{DM} is the focal length associated with the DM shape and n is the index of refraction in the sample [3]. The axial shift is thus related to the DM stroke S by:

$$Z = \frac{4n^3}{NA^2}\left(\frac{R_p}{R_{DM}}\right)S \qquad (1)$$

where NA is the numerical aperture of the microscope objective, R_p is the radius of the objective pupil as imaged onto the DM plane, and R_{DM} is the radius of the active area on the DM. If f_2 is chosen such that $R_p = R_{DM}$,

applying a maximum stroke excursion of ΔS results in an EDOF given by $D = 4n^3\Delta S/NA^2$. Since a standard wide-field microscope has a DOF approximately given by $D_0 = n\lambda/NA^2$, the DM extends the DOF by a factor of $D/D_0 = 4n^2\Delta S/\lambda$.

3. Deconvolution

A difficulty with wide-field microscopy is that it does not provide optical sectioning. That is, in-focus images are generally contaminated with out-of-focus background. The same is true when extending the DOF of a widefield microscope. All-in-focus images become contaminated with all-out-of-focus background, leading to a background haze that worsens as D increases. A strategy to mitigate this problem of background haze is to use deconvolution. The corresponding representative extended 2D optical transfer function (or EOTF) required for deconvolution can be derived directly from the 3D OTF, taking advantage of the fact that the 3D OTF can be expressed analytically under the paraxial approximation for a circular unobstructed pupil. We adapt this expression from [4]:

$$OTF(\vec{k}_\perp, k_z) = \frac{4k}{\pi k_\perp \Delta k_\perp}\sqrt{1-\left(\frac{2k|k_z|}{k_\perp \Delta k_\perp}+\frac{k_\perp}{\Delta k_\perp}\right)^2} \tag{2}$$

where k = n/λ is the wavenumber and $\Delta k_\perp$=2NA/λ is the pupil bandwidth. Eq. 2 is valid for lateral spatial frequencies in the range $|\vec{k}_\perp| = k_\perp \le \Delta k_\perp$, and axial spatial frequency in the range $k_z \le \frac{k_\perp}{2k}(\Delta k_\perp - k_\perp)$; otherwise it is zero. Furthermore, it is normalized so that $\int OTF(\vec{k}_\perp, k_z)\,\mathrm{d}k_z$, which corresponds to the in-focus 2D OTF, is equal to unity when $k_\perp \to 0$.

To derive a representative EDOF associated with an axial scan range D we first take an inverse Fourier transform of the 3D OTF with respect to k_z, as described in [5], and then average this over the scan range, obtaining

$$EOTF(\vec{k}_\perp, D) = \int_{-D/2}^{D/2}\frac{\mathrm{d}z}{D}\int \mathrm{d}k_z e^{i2\pi k_z z} OTF(\vec{k}_\perp, k_z) = \int \mathrm{d}k_z \mathrm{sinc}(k_z D) OTF(\vec{k}_\perp, k_z) \tag{3}$$

This expression is exact, however its numerical integration is not always straightforward. We thus adopt a few approximations. We consider the limit of $D \to 0$ and $D \to \infty$. In the first case we have the 2D in-focus OTF, and in the second we can take k_z in Eq. 2. Since the frequency support can be no better than the in-focus OTF, and Eq. 3 diverges for $D \to \infty$, we can approximate the EOTF as the minimum of the two limits:

$$EOTF(\vec{k}_\perp, D) \approx \min\begin{cases}\frac{2}{\pi}\left(\cos^{-1}(\eta) - \eta\sqrt{1-\eta^2}\right) \\ \frac{4k}{\pi D \Delta k_\perp{}^2 \eta}\sqrt{1-\eta^2}\end{cases} \tag{4}$$

Where $\eta = k_\perp/\Delta k_\perp$. This provides good agreement with the exact integration of Eq. 3 for both large and small values of D, as seen in Fig. 2.

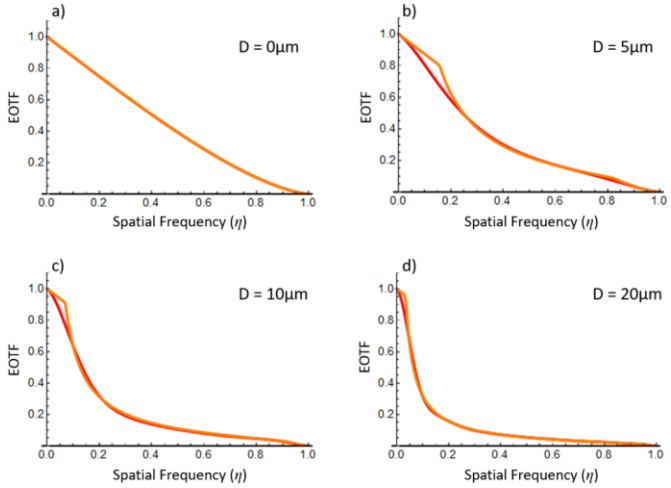

Fig 2. Magnitude of EDOF for different scan ranges. Approximation (orange) of EDOF magnitude obtained from Eq. 4 gives good agreement with "exact" curve (red) obtained by numerical integration of Eq. 3.

Since the EOTF approaches zero for large values of $k_\perp$, and additional modification must be made to regularize the small EOTF at high spatial frequency. We therefore obtain the object using the equation [6]:

$$O(\vec{x}) = F^{-1}\left[\frac{EOTF^*(\vec{k}_\perp,D)}{\left|EOTF(\vec{k}_\perp,D)\right|^2+\varepsilon}F[I(\vec{x})]\right] \quad (5)$$

Where F corresponds to a Fourier transform and $0 \leq \varepsilon \ll 1$ is the regularization parameter. The resulting image shows a marked improvement over the simple EDOF image, as seen in Fig. 3.

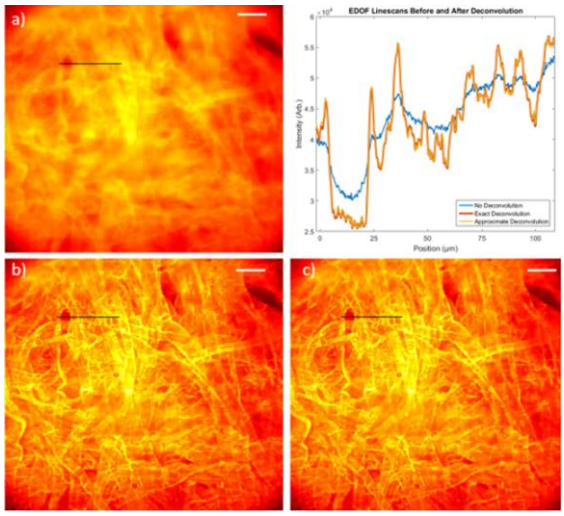

Fig 3. EDOF images of stained tissue paper. Plain EDOF image (a) shows poor contrast and resolution. Deconvolution using both the numerically integrated EDOF (b) and the approximation (c) give significantly improved imaging, and are in good agreement with each other.

4. Anticipated Results

We will be presenting images and videos of live neurons in the brain of a mouse, at video rate. The necessity of an accurate deconvolution kernel will be demonstrated as well.

5. Acknowledgements

We acknowledge the support of the National Science Foundation Industry/University Cooperative Research Center for Biophotonic Sensors and Systems (IIP-1068070) and the National Institute of Health (R01CA182939). We also thank Lei Tian and Anne Sentenac for helpful discussions. Brain tissue samples were supplied by the Jason Ritt laboratory. Professor Bifano acknowledges a financial interest in Boston Micromachines Corporation.

[1] Y. Gong, C. Huang, J. Z. Z. Li, B. F. Grewe, Y. Zhang, S. Eismann, and M. J. Schnitzer, "High-speed recording of neural spikes in awake mice and flies with a fluorescent voltage sensor." Science **350**, 1361–1366 (2015).

[2] N. Ji, J. Freeman, and S. L. Smith, "Technologies for imaging neural activity in large volumes," Nature Neuroscience **19**, 1154–1164 (2016).

[3] J. D. Giese, T. Ford, and J. Mertz, "Fast volumetric phase-gradient imaging in thick samples," Optics Express **22**, 1152–1162 (2014)

[4] B. Frieden, "Optical Transfer of the Three-Dimensional Object," J. Opt. Soc. Am. **57**, 56–66 (1967).

[5] C. Sheppard and M. Gu, "Approximation to the three-dimensional optical transfer function," J. Opt. Soc. Am. A **8**, 692–694 (1991).

[6] S.-H. Lu and H. Hua, "Imaging properties of extended depth of field microscopy through single-shot focus scanning." Optics Express **23**, 10714–10731 (2015).